

# Power Loading in Parallel Diversity Channels Based on Statistical Channel Information

Justin P. Coon, *Senior Member, IEEE*, and Rafael Cepeda, *Senior Member, IEEE*

**Abstract**—In this paper, we show that there exists an arbitrary number of power allocation schemes that achieve capacity in systems operating in parallel channels comprised of single-input multiple-output (SIMO) Nakagami- $m$  fading subchannels when the number of degrees of freedom  $L$  (e.g., the number of receive antennas) tends to infinity. Statistical waterfilling – i.e., waterfilling using channel statistics rather than instantaneous channel knowledge – is one such scheme. We further prove that the convergence of statistical waterfilling to the optimal power loading scheme is at least  $\mathcal{O}(1/(L \log L))$ , whereas convergence of other schemes is at worst  $\mathcal{O}(1/\log L)$ . To validate and demonstrate the practical use of our findings, we evaluate the mutual information of example SIMO parallel channels using simulations as well as new measured ultrawideband channel data.

**Index Terms**—Capacity, power loading, diversity, statistical channel state information, Nakagami- $m$ , UWB.

## I. INTRODUCTION

Parallel channels are frequently encountered in modern communication systems. Examples of such systems include those using orthogonal frequency division multiplexed (OFDM) transmissions, time-division multiplexed (TDM) transmissions, frequency-hop spread-spectrum (FH-SS), and multiple-input multiple-output (MIMO) systems that employ eigenmode transmission techniques.

In recent years, the design of subchannel power allocation strategies has become a popular research topic for systems operating in parallel channels. Power loading schemes based on having perfect channel state information at the transmitter (CSIT) have been developed to maximize spectral efficiency [1] and system throughput [2], as well as to minimize bit-error rate [3], [4] and transmit power [5]. Solutions that rely on partial CSIT have also been devised (see, e.g., [6]).

Here, we investigate power loading in parallel channels using only *statistical* CSIT (SCSIT). Several researchers have reported notable results on the use of SCSIT in the literature. For example, power loading based on SCSIT to minimize bit-error rate was studied in [7], while in [8], the authors developed power and bit allocation algorithms to maximize the spectral efficiency and minimize the power consumption. More recently, in [9], the authors investigated transmission in jointly correlated MIMO channels, whereby the transmit vector is conveyed over the eigenmodes of the transmit correlation

matrix, and power allocation is performed to maximize an upper bound on the ergodic capacity. It was found that, for parallel channels in particular, *statistical waterfilling* – i.e., waterfilling using the *mean* channel gains instead of the *instantaneous* gains – optimized this bound [9, cf. (67)].

In this paper, we study power loading in parallel channels comprised of single-input multiple-output (SIMO) subchannels where the number of degrees of freedom of each subchannel (e.g., the number of receive antennas) is denoted by  $L$ . We maintain generality in our analysis by assuming the single-input single-output (SISO) channels that constitute each SIMO subchannel adhere to a Nakagami- $m$  fading model. In contrast to [9], we investigate conditions under which we can determine the power loading schemes that maximize the *exact* ergodic capacity of such a parallel channel rather than an upper bound. To this end, we show that as  $L \rightarrow \infty$ , there are arbitrarily many such schemes, where statistical waterfilling is one such approach. Furthermore, we demonstrate that convergence to the optimal power allocation scheme is  $\mathcal{O}(1/(L \log L))$  for statistical waterfilling, whereas the convergence of other asymptotically optimal schemes is at worst  $\mathcal{O}(1/\log L)$ . Finally, we validate and demonstrate the practical use of our findings through a study of SIMO parallel channels using simulations as well as new measured ultrawideband (UWB) channel data.

The rest of the paper is organized as follows. Bounds on the capacity of a parallel channel are given in Section II. These bounds are used to develop the main results on the asymptotic optimality and convergence properties of statistical waterfilling and other power loading strategies in SIMO systems in Section III. Measured and simulated channel data are used to measure performance in Section IV, and conclusions are then drawn in Section V.

## II. BOUNDS ON CAPACITY

Consider a parallel channel comprised of  $N$  SIMO subchannels, each with  $L$  degrees of freedom<sup>1</sup>. The mutual information<sup>2</sup> of the  $n$ th subchannel, assuming full channel state information is available at the receiver, is given by [10]

$$I_{\gamma_n}(P_n) = \log \left( 1 + \frac{P_n}{N_0} \gamma_n \right)$$

where  $\gamma_n = \|\mathbf{h}_n\|^2$  with  $\mathbf{h}_n \in \mathbb{C}^L$  being a vector of complex channel coefficients,  $P_n$  is the power transmitted on this

<sup>1</sup>The restriction that all subchannels have  $L$  degrees of freedom is made for simplicity of presentation; in fact, the main result of this paper holds even if  $L$  varies across the subchannels.

<sup>2</sup>Mutual information and capacity are defined in units of nats.

J. P. Coon is with Toshiba Research Europe Ltd., 32 Queen Square, Bristol, BS1 4ND, UK; tel: +44 (0)117 906 0700, fax: +44 (0)117 906 0701, email: justin@toshiba-trel.com.

R. Cepeda was with Toshiba Research Europe Ltd. and is now with British Sky Broadcasting Ltd., Grant Way, Isleworth, Middlesex, TW7 5QD, UK; tel: +44 (0)20 7032 7752, fax: +44 (0)20 7900 7161, email: rafael.cepeda@bskyb.com.

subchannel, and  $N_0$  is the variance of the zero-mean, additive white Gaussian noise on that subchannel<sup>3</sup>. It follows that the ergodic capacity of the parallel channel is given by

$$C = \sup_{\substack{P_n \geq 0, \\ \sum P_n = P}} \left\{ \sum_{n=1}^N E[I_{\gamma_n}(P_n)] \right\}. \quad (1)$$

Since only SCSIT is available, the powers  $\{P_n\}$  cannot be functions of  $\{\gamma_n\}$ , but instead rely upon the statistics of these channel gains. We define the set  $\{P_n^*\}$  as the set of optimal powers, i.e., the set that yields the supremum given above.

To develop our main results, we will require an upper and a lower bound on  $C$ . An upper bound is easily calculated using Jensen's inequality. Let  $P_n^s$  denote the power loading strategy based on statistical waterfilling, which is given by

$$P_n^s = \left( \nu - \frac{N_0}{\mu_n} \right)^+ \quad (2)$$

where  $(x)^+ = \max\{0, x\}$ ,  $\mu_n = E[\gamma_n]$  is the mean of the  $n$ th subchannel gain, and  $\nu$  is chosen to satisfy  $\sum P_n^s = P$ . Now, we can write

$$C \leq \sum_{n=1}^N I_{\mu_n}(P_n^*) \leq \sum_{n=1}^N I_{\mu_n}(P_n^s) \quad (3)$$

where the first inequality follows from the concavity of  $I$  and the second results from the standard waterfilling solution.

Clearly,  $\{P_n^s\}$  is not the only set that satisfies this bound; it is simply the set that *maximizes* the bound. It will be convenient to define another set of powers  $\{P_n'\}$  that satisfies

$$C \leq \sum_{n=1}^N I_{\mu_n}(P_n') \leq \sum_{n=1}^N I_{\mu_n}(P_n^s) \quad (4)$$

such that  $\sum P_n' = P$ . Note, we do not explicitly define  $\{P_n'\}$ .

For the lower bound, we begin with the trivial inequality

$$C \geq \sum_{n=1}^N E[I_{\gamma_n}(P_n')]. \quad (5)$$

Applying Markov's inequality yields the more useful bound

$$C \geq \sum_{n=1}^N a_n \mathcal{F}_n \left( \frac{N_0}{P_n'} (e^{a_n} - 1) \right) \quad (6)$$

where  $\mathcal{F}_n(x) = \Pr(\gamma_n \geq x)$  is the complementary cumulative distribution function (CCDF) of the  $n$ th subchannel gain and  $a_n > 0$ . Note that a sufficient (but not necessary) condition for this bound to hold is  $P_n' = P_n^s$  for all  $n$ .

### III. POWER LOADING IN DIVERSITY CHANNELS

We now present our main results. We consider the case where each subchannel experiences Nakagami- $m$  fading. The constituent single-input single-output (SISO) channels corresponding to the  $n$ th SIMO subchannel are statistically independent, and the  $\ell$ th SISO channel gain, denoted by  $|h_{n,\ell}|^2$ , is gamma distributed with scale parameter  $\theta_n$  and shape

parameter  $m_n$ . Note that we assume the scale and shape parameters are identical for all SISO channels that constitute the  $n$ th subchannel. Thus, the channel gain  $\gamma_n = \|\mathbf{h}_n\|^2$  is a gamma distributed variate with scale parameter  $\theta_n$  and shape parameter  $m_n L$ . The density function of  $\gamma_n$  is given by

$$f_n(\gamma) = \frac{\gamma^{m_n L - 1} e^{-\frac{\gamma}{\theta_n}}}{\theta_n^{m_n L} \Gamma(m_n L)}, \quad \gamma \geq 0. \quad (7)$$

The mean of the  $n$ th subchannel gain in this case is given by

$$\mu_n = \theta_n m_n L \quad (8)$$

Now we can study the capacity as the number of degrees of freedom  $L$  grows large, which leads to the following proposition.

*Proposition 1:* Consider a parallel channel with subchannel gains distributed according to (7). In the limit of large  $L$ , there are arbitrarily many asymptotically optimal power loading strategies, one of which is the statistical waterfilling solution defined by (2).

*Proof:* We prove the proposition by showing that the upper and lower bounds given by

$$\sum_{n=1}^N E[I_{\gamma_n}(P_n')] \leq C \leq \sum_{n=1}^N I_{\mu_n}(P_n') \quad (9)$$

are asymptotically equivalent (as  $L \rightarrow \infty$ ) for any set  $\{P_n'\}$  that satisfies (9) for  $L > L_0$ . Note that we do not explicitly define  $\{P_n'\}$ , although it is clear that one possible definition is  $P_n' = P_n^s$  for all  $n$  since this definition satisfies (9) for all  $L$ . We first consider the upper and lower bounds on the capacity of the  $n$ th subchannel. We assume that a nonzero power is allocated for transmission on this subchannel; this is a valid assumption since if the converse were true, the upper and lower bounds on capacity would both be zero. The CCDF of the  $n$ th subchannel gain is

$$\mathcal{F}_n(x) = Q\left(m_n L, \frac{x}{\theta_n}\right) \quad (10)$$

where  $Q(a, x) = \Gamma(a, x)/\Gamma(a)$  is the normalized upper incomplete gamma function. Now, letting  $\beta_n = P_n' \theta_n m_n / N_0$  where  $P_n' > 0$ , we can write the ratio of the lower and upper bounds given by (6) and (4), respectively, as a function of  $L$ :

$$r_L = \frac{a_n Q(m_n L, \beta_n^{-1} m_n (e^{a_n} - 1))}{\log(1 + \beta_n L)}. \quad (11)$$

For every  $L \in \mathbb{N}$  and  $n \in \{1, 2, \dots, N\}$ , we can calculate  $\beta_n$ . Thus, we can choose to define

$$a_n = \log(1 + \alpha \beta_n L) > 0 \quad (12)$$

where  $0 < \alpha < 1$ . It follows that

$$r_L = \frac{\log(1 + \alpha \beta_n L)}{\log(1 + \beta_n L)} Q(m_n L, \alpha m_n L). \quad (13)$$

Using [11, 5.11.3] and [11, 8.11.6], and noting that  $0 < \alpha e^{1-\alpha} < 1$  for  $0 < \alpha < 1$ , we can expand  $r_L$  at  $\infty$  to

<sup>3</sup>We assume without loss of generality that the power spectral densities of the noise processes on all subchannels are identical.

obtain

$$r_L = \underbrace{\left(1 + \frac{\log \alpha}{\log L} + \mathcal{O}\left(\frac{1}{(\log L)^2}\right)\right)}_{\text{logarithmic term}} \times \underbrace{\left(1 - \frac{(\alpha e^{1-\alpha})^{m_n L}}{(1-\alpha)\sqrt{2\pi m_n L}}(1 + \mathcal{O}(L^{-1}))\right)}_{\text{gamma function term}}. \quad (14)$$

Thus,  $r_L \rightarrow 1$  as  $L \rightarrow \infty$ . Since this relation holds for any  $n$ , the upper and lower bounds given in (9) are asymptotically equivalent, and  $\{P'_n\}$  is an optimal set of powers. Finally, it follows from continuity that any set  $\{P'_n + \epsilon_n\}$  with  $\epsilon_n \in \mathbb{R}$ , which satisfies (9), is also optimal.  $\square$

This result can be understood intuitively by noting that the mean channel gains increase monotonically with the number of degrees of freedom  $L$ . Thus, the effective SNR on a given subchannel grows without bound as  $L \rightarrow \infty$ , suggesting that an equal power allocation strategy is optimal. Many power loading strategies satisfy this condition, including traditional waterfilling and statistical waterfilling. In fact, this result is also related to the notion of “channel hardening”, which has been studied in the information theoretic literature. In particular, our result is corroborated by related findings detailed recently in [12, cf. §IV].

Proposition 1 is stronger than it may first appear since it implies that one may theoretically determine the number of diversity branches such that, when an asymptotically optimal power loading strategy is employed, the ergodic capacity can be approached to an arbitrarily close degree. More exactly, for arbitrarily small  $\epsilon > 0$ , there exists some positive integer  $L_0$  such that when  $L > L_0$  we have  $|C - C'| < \epsilon$ , where  $C'$  denotes the rate obtained by employing the suboptimal power allocation scheme  $\{P'_n\}$ .

Although we have demonstrated the asymptotic optimality of an arbitrary number of power loading schemes, including statistical waterfilling, it is essential from a practical viewpoint that we understand the convergence behavior of this result. Convergence can be studied by observing the rate at which the upper and lower bounds on capacity, given by (9), approach the limit in  $L$ . This leads to our second main result.

**Proposition 2:** Statistical waterfilling converges to the optimal power loading strategy like  $\mathcal{O}(1/(L \log L))$ , whereas for more general asymptotically optimal power loading strategies, convergence is, at worst,  $\mathcal{O}(1/\log L)$ .

*Proof:* The proof of the first part follows by substituting  $P'_n = P_n^s$  in the expression for  $r_L$  given by (13) and expanding at  $L = \infty$ . The second part follows from the proof of Proposition 1).  $\square$

From this proposition, we see that although there are arbitrarily many asymptotically optimal power loading strategies, convergence to optimality is guaranteed to be significantly faster for statistical waterfilling than for general schemes. Consequently, statistical waterfilling is not only easily implemented and intuitive, but is a practical solution for systems with moderate levels of inherent diversity.

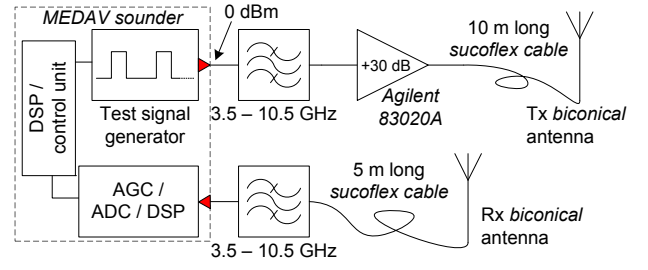


Fig. 1. Interconnection of sounding equipment.

#### IV. NUMERICAL EVALUATION

One example of a parallel channel with subchannels that experience unequal mean fading gains can be found in OFDM-based UWB systems. In this section, we evaluate our findings by considering both measured and simulated UWB channels.

##### A. Measured Channels

A channel measurement campaign was conducted using a state-of-the-art  $2 \times 4$  time-domain multi-antenna UWB channel sounder. The sounder, manufactured by MEDAV, interrogates the propagation channel by using trains of pseudo noise (PN) sequences of 4095 pulses or chips [13]. These are generated in baseband at a clock rate of 6.95 GHz and later up-converted, using the same clock, to cover the bandwidth from approximately 3.5 to 10.5 GHz. In turn, the receiver down-converts captured signals, does a periodic sub-sampling of them, and uses a phase shifter to allow the sampling of complex channel impulse responses (CIRs) in the time domain.

Fig. 1 shows the configuration of the sounding equipment for measurements. Test signals are generated and bandpass filtered to avoid out-of-band emissions. The test signals are then amplified, transferred to a biconical antenna for radiation and, after travelling through the propagation environment, received by a similar antenna connected to a bandpass filter [14], [15]. After correcting the gain of the incoming signals with an automatic gain control (AGC) unit, the receiver uses an analogue-to-digital converter (ADC) and performs a matched filtering of the data, with the known PN sequence, in a digital signal processing (DSP) unit. Before sounding and after a warming-up period, the system response, phase imbalance and crosstalk are characterized using cabled or open connections. These measured parameters are then used for calibration to leave only the combined response of the antennas and the environment on the data recordings.

UWB ( $2 \times 4$ ) MIMO channel measurements were conducted in an open-plan modern office in the central area of Bristol, UK. The sounding environment had typical scattering objects such as personal computers, liquid crystal displays (LCDs), non-metallic cubicle partitions, desks and metallic cabinets. The ceiling of the office was made of perforated metallic tiles and the floor supported by a metallic structure covered with non-metallic material. The dimensions of the sounded office are: 12.74 m wide, 30.84 m long and 2.39 m high.

For this work, each recorded CIR results from averaging 256 captured CIRs in hardware. Under these conditions, the

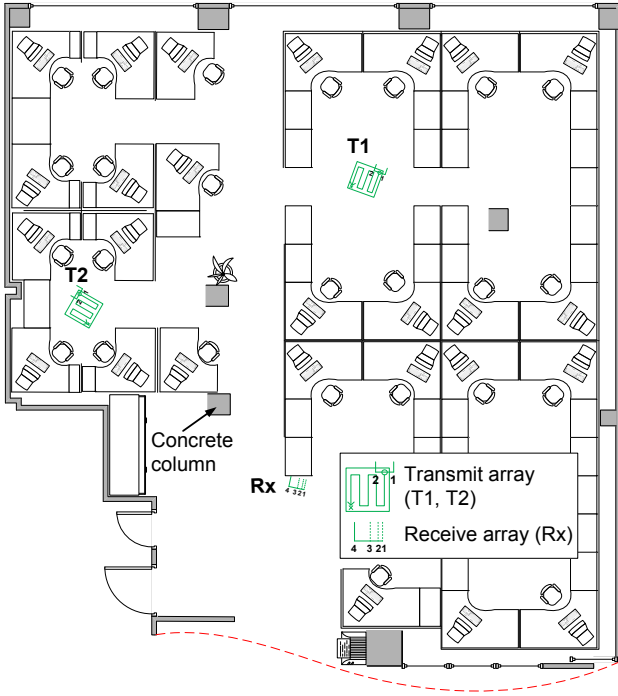


Fig. 2. Illustration of sounded environment and antenna locations.

observation time of the system for a recorded CIR is 155 ms. The antennas were mounted on fibreglass masts at 1.3 m from the floor. The transmit antenna mast was attached to the movable part of an  $x - y$  automated positioning system [16]. The positioners and the sounder were remotely controlled to prevent human intervention in the area of measurements. In parallel, a spectrum analyzer, connected to a biconical antenna and a low noise amplifier, periodically scanned the spectrum of interest. This information was used to check the “health” of the test signal and the presence of interfering signals.

Fig. 2 shows a diagram of the sounded environment. Two specific locations were selected to capture line-of-sight (LOS) and non-line-of-sight (NLOS) data. These locations, T1 (LOS) and T2 (NLOS), are grids of  $x - y$  points in which two transmit antennas, 25 cm apart, were displaced at distances of 3 cm. The receive antenna mast was positioned at a fixed location (Rx), and a four-element linear antenna array was formed by securing the first antenna and the following ones at 3, 6 and 12 cm from it. Each measurement grid had 441 ( $21 \times 21$ ) points, so a total of 3528 ( $441 \times 8$ ) CIRs were recorded for each location T. In general, the distance between transmit and receive antennas ranges from approximately 7.02 m to 6.51 m for T1 and from 6.41 m to 5.77 m for T2. Note that NLOS conditions were achieved by locating the transmit antenna in such a way that a concrete column was always shadowing it from the receive one.

SIMO channels are formed by extracting the CIRs measured from the first transmit antenna to the receive antennas spaced apart by 12 cm distance. Each of these CIR is converted into the frequency domain, by using a discrete Fourier transform (DFT), and we retain the channel frequency response characteristics for the 5-to-6 GHz band. With a frequency spacing

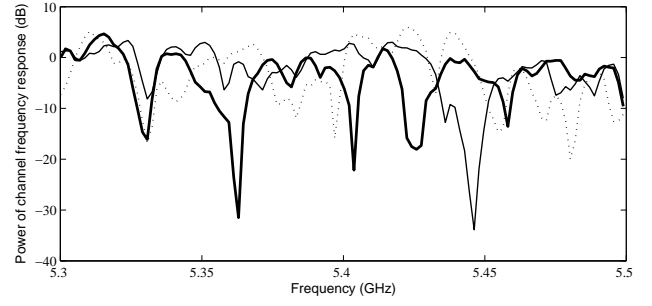


Fig. 3. Plot of the power of three consecutive channel frequency response measurements in the 5.3-to-5.5 GHz band.

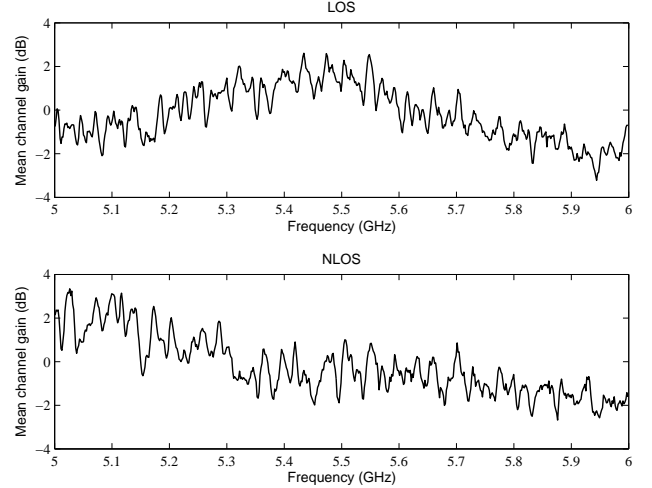


Fig. 4. Mean channel gains for LOS and NLOS measured channels in the 5-to-6 GHz band.

of roughly 1.7 MHz, this amounts to 588 frequency samples, i.e., channel frequency response coefficients. A power plot of three consecutive NLOS measurements in the 5.3-to-5.5 GHz band is illustrated in Fig. 3. From this figure, we can see that the measurements are fairly independent of one another.

The channel measurements were normalized such that the average mean channel gain (in frequency) is one. Fig. 4 depicts the mean channel gain (averaged over the 441 available snapshots) for the LOS and NLOS channels. It is certainly clear from this figure that the mean fading gains vary considerably with frequency. Thus, one would expect an unequal power loading strategy based on the statistics of these channels to perform better than a balanced power allocation scheme.

In Fig. 5, bounds on the capacity, defined by (3) and (5), are plotted for the measured LOS and NLOS channels. Additionally, the mutual information for a channel where a balanced power allocation is used is illustrated. The lower bound and the balanced power rate are both averaged over the 441 snapshots of measured data to emulate the expectation in the rate expression. Since a large range of SNR values are considered in these graphs, it is beneficial, for ease of comparison, to normalize these results with respect to the capacity of a parallel additive white Gaussian noise (AWGN) channel. It is evident from Fig. 5 that statistical waterfilling is capable of providing significant gains at low SNR, which

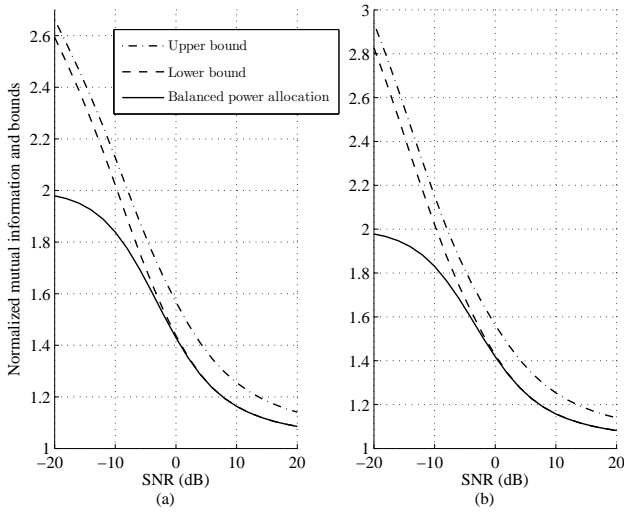


Fig. 5. Normalized mutual information (w.r.t. a parallel AWGN channel) and bounds for measured LOS channels (a) and NLOS channels (b).

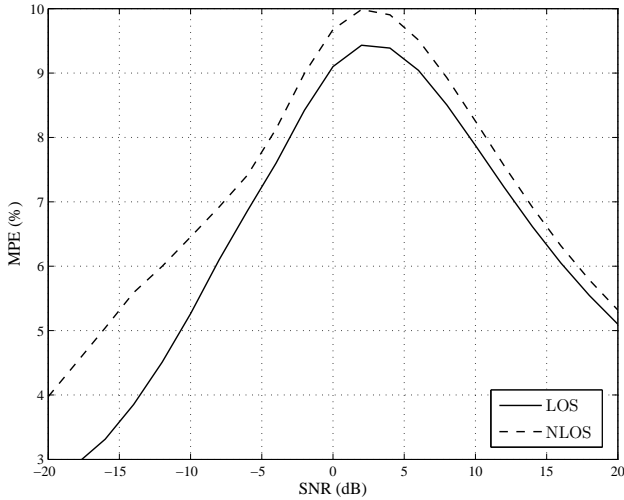


Fig. 6. MPE for measured LOS and NLOS channels.

exemplifies typical operating conditions in wideband systems with a strict power budget, such as UWB.

It is also useful to examine the *maximum percent error* (MPE) of the capacity bounds, which is defined as  $MPE = 100\% \times (C_{UB} - C_{LB}) / C_{LB}$  where  $C_{UB}$  and  $C_{LB}$  are the upper and lower bounds given by (3) and (5), respectively. This metric quantifies the deviation of the statistical waterfilling power allocation strategy from the optimal power allocation since the power-optimal rate lies between  $C_{LB}$  and  $C_{UB}$ . The MPE is illustrated in Fig. 6, which shows that even for the practical situation of  $L = 4$ , the difference in the two bounds is relatively small, from which we deduce that statistical waterfilling is a good pragmatic power loading strategy.

### B. Simulated Channels

In the measured scenario, we are limited to studying the mutual information of a SIMO channel with  $L \leq 4$  receive antennas. Thus, we employ simulations to observe the perfor-

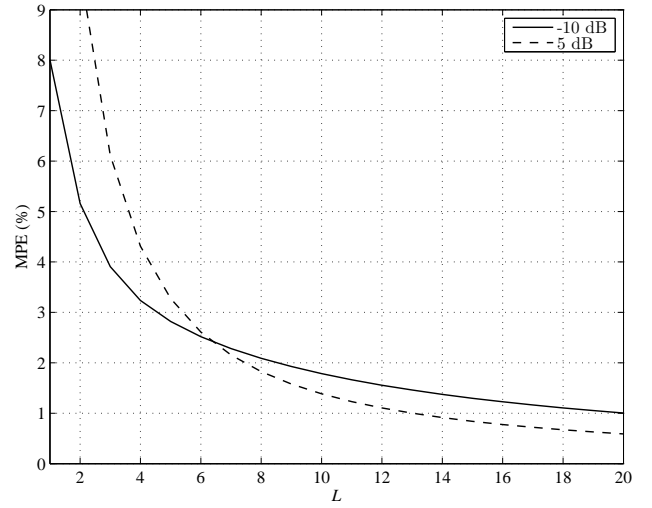


Fig. 7. MPE for measured LOS and NLOS channels.

mance of various power loading strategies as a function of  $L$ . To this end, we consider a system operating in the 5-to-6 GHz band as above, but where the mean channel gain decays with frequency like  $f^3$ , which is typical in rich scattering environments.

We are particularly interested in the MPE of the upper and lower capacity bounds, and plot this metric in Fig. 7 as a function of  $L$  for SNR values of  $-10$  dB and  $5$  dB. This figure confirms that statistical waterfilling converges to the optimal power loading strategy quickly, achieving an MPE of less than 5% for  $L \geq 4$ , thus making this technique suitable for many practical systems.

## V. CONCLUSIONS

In this paper, we showed that there exist an arbitrary number of power loading strategies that achieve capacity for parallel channels comprised of SIMO subchannels in the limit of a large number of degrees of freedom  $L$ . Statistical waterfilling was shown to be one such strategy, which in fact is guaranteed to converge to the optimal solution much quicker than other asymptotically optimal solutions. We demonstrated the practicality of our results through a study of measured and simulated UWB channels.

## REFERENCES

- [1] M. Lei, P. Zhang, H. Harada, and H. Wakana, "An adaptive power distribution algorithm for improving spectral efficiency in OFDM," *IEEE Trans. Broadcast.*, vol. 50, no. 3, pp. 347–351, Sep. 2004.
- [2] G. Bansal, M. J. Hossain, and V. K. Bhargava, "Optimal and suboptimal power allocation schemes for OFDM-based cognitive radio systems," *IEEE Trans. Wireless Commun.*, vol. 7, no. 11, pp. 4710–4718, Part/Nov. 2008.
- [3] L. Goldfeld, V. Lyandres, and D. Wulich, "Minimum BER power loading for OFDM in fading channel," *IEEE Trans. Commun.*, vol. 50, no. 11, pp. 1729–1733, Nov. 2002.
- [4] N. Y. Ermolova and B. Makarevitch, "Power loading for OFDM with incomplete channel state information," in *Personal, Indoor and Mobile Radio Communications, 2007. PIMRC 2007. IEEE 18th International Symposium on*, Sep. 3–7, 2007, pp. 1–5.
- [5] K. Liu, F. Yin, W. Wang, and Y. Liu, "Efficient adaptive loading algorithm with simplified bandwidth optimization method for OFDM systems," in *Global Telecommunications Conference, 2005. GLOBE-COM '05. IEEE*, vol. 5, St. Louis, MO, Dec. 2–2, 2005.

- [6] M. Vu and A. Paulraj, "On the capacity of MIMO wireless channels with dynamic CSIT," *IEEE J. Sel. Areas Commun.*, vol. 25, no. 7, pp. 1269–1283, Sep. 2007.
- [7] F. F. Digham and M. O. Hasna, "Performance of OFDM with m-QAM modulation and optimal loading over rayleigh fading channels," in *Vehicular Technology Conference, 2004. VTC2004-Fall. 2004 IEEE 60th*, vol. 1, Sep. 26–29, 2004, pp. 479–483.
- [8] Z. Song, K. Zhang, and Y. L. Guan, "Joint bit-loading and power-allocation for OFDM systems based on statistical frequency-domain fading model," in *Vehicular Technology Conference, 2002. Proceedings. VTC 2002-Fall. 2002 IEEE 56th*, vol. 2, Sep. 24–28, 2002, pp. 724–728.
- [9] X. Gao, B. Jiang, X. Li, A. Gershman, and M. McKay, "Statistical eigenmode transmission over jointly correlated MIMO channels," *IEEE Trans. Inf. Theory*, vol. 55, no. 8, pp. 3735–3750, Aug. 2009.
- [10] D. Tse and P. Viswanath, *Fundamentals of Wireless Communication*. Cambridge University Press, 2005, available online.
- [11] F. W. J. Olver, Ed., *NIST Handbook of Mathematical Functions*. Cambridge University Press, 2010.
- [12] D. Bai, P. Mitran, S. Ghassemzadeh, R. Miller, and V. Tarokh, "Rate of channel hardening of antenna selection diversity schemes and its implication on scheduling," *IEEE Trans. Inf. Theory*, vol. 55, no. 10, pp. 4353–4365, Oct. 2009.
- [13] J. Sachs, R. Herrmann, M. Kmec, M. Helbig, and K. Schilling, "Recent advances and applications of m-sequence based ultra-wideband sensors," in *Ultra-Wideband, 2007. ICUWB 2007. IEEE International Conference on*, 24–26 Sept. 2007, pp. 50–55.
- [14] IRK Dresden, (2011, March). [Online]. Available: <http://www.irk-dresden.de/en/>
- [15] R. Cepeda, W. Thompson, and M. Beach, "On the mathematical modelling and spatial distribution of UWB frequency dependency," in *Wideband and Ultrawideband Systems and Technologies: Evaluating current Research and Development, 2008 IET Seminar on*, Nov. 2008, pp. 1–5.
- [16] 402/403/404XE Series Product Manual, Parker Hannifin Corp. September 2006 (2011, March). [Online]. Available: <http://www.compumotor.com/manuals/XE/xeprodmanrev2.pdf>